A Method of Analysis for Propellers at Extreme Angles of Attack

GERALD F. HALL*
The Pennsylvania State University, University Park, Pa.

The method developed analyzes the propeller at extreme angles of attack by considerations on a simplified model of the wake similar to the classical Prandtl model for axial flight. The analysis consists of determining a "tip-loss" factor for the propeller at an angle of attack. This tip-loss factor is, like Prandtl's, a function of the number of blades, nondimensional propeller radius, and wake helix geometry; but a dependence on wake skew angle is also observed. The solution is obtained numerically on an IBM 7074 digital computer. A method of solution to the "direct problem" in propeller aerodynamics utilizing this tip-loss factor is suggested. Thrust and power requirements for an existing propeller are determined and compared with experimental values. Reasonable agreement between theory and experiment is obtained within a practical range of angle of attack α, and the parameter μ (i.e., tip-speed ratio) $\cos\alpha$. However, thrust and power are generally under predicted at low values of $\mu\cos\alpha$ for all angles of attack. Major sources of error are believed due to the relatively simple mathematical model and inaccurate airfoil data in the regions of blade section stall and reverse flow.

Nomenclature

a = normal spacing of slits
a_0 = airfoil section two-dimensional lift curve slope
B = number of blades
b = slit span
c = airfoil chord
C_l = airfoil section lift coefficient
C_d = airfoil section drag coefficient
C_T = propeller thrust coefficient
C_p = propeller power coefficient
F = tip-loss factor
F_0 = tip-loss factor for zero skew angle
r = local propeller radius
$\bar{r}$ = nondimensional radius, r/R
R = propeller radius
T = propeller thrust
V = velocity
v = momentum induced velocity
W = wake induced velocity, also wake impact velocity
x = slit coordinate (vortex location)
$\bar{x}$ = x/a
x_0 = slit coordinate at which induced velocity is determined
$\bar{x}_0$ = x_0/a
α = propeller angle of attack
β = blade pitch angle
γ = running strength of slit vortex sheet
$\bar{\gamma}$ = $\gamma/2\pi W_N$
Γ = circulation
$\bar{\Gamma}$ = $\Gamma/2\pi W_N a$
θ = angular coordinate
μ = tip-speed ratio
σ = local solidity
ϕ = wake helix angle
χ = wake skew angle
ψ = blade azimuth angle

Subscripts

a = axial
e = effective, at a blade element
i = induced
n = summation index
N = normal
0 = zero skew angle; also wake impact velocity
t = tangential
T = tip
u = unsteady
∞ = ultimate wake; also infinite number of blades

Received September 29, 1967; revision received August 12, 1968. The author wishes to express his gratitude to B. W. McCormick Jr. of the Department of Aerospace Engineering for his many helpful suggestions concerning this work.

* Instructor of Aerospace Engineering. Associate Member AIAA.

Introduction

EXTENSIVE application of the propeller as a propulsive device has given rise to a number of techniques for predicting propeller performance. These techniques range from simple momentum theory to the more detailed potential theoretic treatments of Goldstein and Prandtl. Regardless of complexity, however, all early propeller theories consider only the case of a propeller thrusting in its flight direction, with a steady and uniform flow through the disk swept out by the propeller.

These assumptions are obviously unrealistic for rotary wings and V/STOL applications of propellers, since here the propeller provides not only a propulsive force, but a lifting force as well. The thrust vector in this case has an angle of attack, giving rise to a component of the freestream velocity in the plane of the propeller; indeed, for the rotary wing, the full freestream velocity lies in the propeller plane. The problem is further complicated by the fact that the in-plane velocity component varies periodically around the azimuth so that the flow is essentially unsteady.

Momentum methods have been used to analyze the propeller in translation with corrections introduced to account for blade dynamic motions; but, as is typical of such methods, they do not yield detailed descriptions of blade loadings or induced velocities. Some attempts (Ref. 1, for example) to consider this problem with distributed vortices have yielded qualitative insight, but there is some question of their ability to give quantitative estimates of performance.

In the present study, methods are developed for the estimation of pertinent performance parameters for a propeller at a non-negligible angle of attack, i.e., the "direct" problem. A comparison of this method with experimental data given in Ref. 2 is made, and, with certain reservations as discussed, found to be acceptable.

General Assumptions

Before attempting any analysis of the problem, some assumptions with regard to general analytical models of the propeller should be mentioned. For example, the fluid through which the propeller moves is assumed to be an inviscid, homogeneous continuum, and the flowfield is taken to be irrotational.

The propeller blades are assumed to be infinitely rigid with each being replaced by a single bound vortex and an associated trailing vortex wake. This wake consists of an infinite number of trailing vortices of incremental strength springing from radial stations along the blade as a result of the spanwise circulation distribution varying continuously to zero at the blade tip. The trailing wake assumes some general helical shape due to the propeller rotation, with the loops of the wake lying parallel to the propeller disk plane.

It is further assumed the propeller is lightly loaded so that the wake-induced velocity does not affect the wake shape. Hence, the wake trails as a rigid general helical shape in the direction of the wake centerline. Further, since the ultimate wake is a free wake, each vortex filament must trail in a direction specified by the resultant velocity at the radial station from which it springs. The total velocity normal to the filament must then be zero. This boundary condition requires the total velocity normal to the rigid helical wake to be zero.

Thus, if the flow pattern exterior to the rigid helicoid representing the wake can be determined, the discontinuity in potential at a radial position of the wake surface yields directly the bound circulation at that radius. Also, with the potential known, the velocity field is completely described.

Discussion of Prandtl's Analysis for a Propeller in Axial Flight

Prandtl's classical analysis of a propeller in axial flight assumes a propeller with a large number of blades operating at a low advance ratio. The low advance ratio assumption implies that the loops of the helical wake will be nearly flat; that is, the loops of the helical wake are nearly parallel to the propeller disk. The assumption of a large number of blades suggests that the normal distance between two successive sheets will be small with respect to the wake, or propeller radius. With these arguments, the flow exterior to the ultimate vortex wake is nearly identical to the two-dimensional flow past an infinite number of semi-infinite slits.

The propeller bound circulation at a radius r obtained from this model is given as[3]

$$\Gamma = \Gamma_\infty F/B \tag{1}$$

where $F = 2\cos^{-1}[\exp(-\pi x/a)]/\pi$ and $x/a = B(1-\bar{r})/2\pi\sin\phi$. It should be noted that the assumptions of low advance ratio and large number of blades are not as restrictive as they might appear and results of the theory are reasonably accurate over a wide range of advance ratios even for two- and three-bladed propellers.[4,5]

The quantity F is termed the tip-loss factor and can be interpreted as follows. The blade bound circulation at a radius is related to the tangential component of induced velocity in the ultimate wake by

$$B\Gamma = \oint 2W_t(r,\theta)rd\theta \tag{2}$$

where W_t is a function of the radius r and the spacing between blades, θ. If a propeller with an infinite number of blades is considered, the dependency on blade spacing is lost and a circulation for this case can be defined as

$$\Gamma_\infty = \oint 2W_t(r)rd\theta = 4\pi rW_t(r) \tag{3}$$

Writing the bound circulation for a finite blades propeller in the form of Eq. (1) gives

$$F = [\oint 2W_t(r,\theta)rd\theta]/\Gamma_\infty \tag{4}$$

Equation (4) thus indicates that the tip-loss factor is a correction to the bound circulation distribution of an infinite bladed propeller, which accounts for the effect of finite blade spacing. This interpretation and the form of the tip-loss factor given by Eq. (4) will be of importance in developing the analysis of the propeller at an angle of attack.

Note that an approximation to Prandtl's model with semi-infinite slits is a simplification of a wake approximated by slits of finite length. It is by the symmetry of the bound circulation distribution about the propeller axis of rotation (which coincides with the wake centerline) that Prandtl is able ultimately to shift the centerline to infinity and obtain the conformal transformation by which the problem is solved.

Analysis of the Propeller at Extreme Angles of Attack

It would appear from the discussion of the propeller in axial flight that if an equivalent tip-loss factor for the propeller at an angle of attack can be determined, the blade bound circulation distribution and corresponding induced velocity can be realistically approximated. However, to obtain this equivalent tip-loss factor a justification for its existence must be made and a physical model then has to be constructed for analysis.

The necessary justification for the existence of the tip-loss factor can be established as follows. As in axial propeller theory, the total bound circulation at any radius of a B-bladed propeller is given by the closed line integral of the tangential induced velocity in the ultimate wake;

$$\Gamma_{\text{TOT}} = \oint 2W_t(r,\alpha,\theta,t)rd\theta \tag{5}$$

The path of integration is taken in a plane parallel to the propeller disk. Note that in general the tangential induced velocity is a function of radius r, angle of attack α, blade spacing θ, and unsteady character of the flow, t. Equation (5) could have been expressed in terms of the azimuth angles ψ since azimuth angle and time are related through the propeller rotation. Now assume a rigid, nonflapping blade, which is consistent with the Prandtl-Goldstein model of axial flight,[5] and neglect the blade shed vorticity. Then at a radius r of the nth blade the bound circulation can be written as[6]

$$\Gamma_n = \Gamma_0 + \Gamma_1\sin\psi_n \tag{6}$$

where Γ_0,Γ_1 are functions of (r,α). Thus, the total bound circulation for B-blades is

$$\Gamma_{\text{TOT}} = B\Gamma_0 + \Gamma_1\sum_{n=1}^{B}\sin\psi_n \tag{7}$$

If the blades are symmetrically spaced

$$\psi_n = \psi_{\text{REF}} + (2\pi/B)(n-1)$$

so that

$$\Gamma_{\text{TOT}} = B\Gamma_0 \tag{8}$$

and Eq. (4) becomes just

$$B\Gamma_0 = \oint 2W_t(r,\alpha,\theta,t)rd\theta \tag{9}$$

Since the left-hand side of Eq. (9) is independent of time, the closed line integral can be obtained by considering just the steady velocities in the wake and Eq. (9) becomes

$$B\Gamma_0 = \oint 2W_t(r,\alpha,\theta)rd\theta \tag{10}$$

Now, if the number of blades becomes infinite, the circulation becomes some value Γ_∞ and the induced velocity loses its dependence on blade spacing, so that for this condition

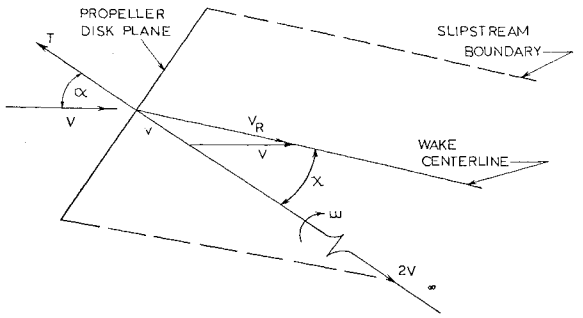

Fig. 1 Force and velocity geometry for analysis of propeller by momentum methods.

Eq. (10) reduces to

$$\Gamma_\infty = 4\pi r W_t(r,\alpha) \tag{11}$$

In general, then, the steady-state bound circulation at some radius of the propeller at an angle of attack can be written

$$\Gamma_0 = \Gamma_\infty F/B \tag{12}$$

where $F = (\oint 2W_t(r,\alpha,\theta)rd\theta)/\Gamma_\infty$.

Thus, for the propeller at an angle of attack, an equivalent tip-loss factor that accounts for the effect of finite blade spacing on the bound circulation distribution can be defined. The only difference between Eqs. (12) and (4) is that the terms in (12) show a dependency on angle of attack. Note also that the problem has been effectively reduced from an unsteady to steady flow problem.

Because the propeller thrusts along the axis of rotation, the flow is accelerated parallel to this direction. The resultant velocity at the center of the disk is then the vector sum of the freestream and propeller-induced velocities. Since the wake is a free wake, the wake centerline that traces the geometric center of the wake must necessarily align itself with this resultant velocity and it is thus skewed at some angle to the axis of rotation. Because the induced velocity accelerates to twice its disk plane value in the ultimate wake, the skew angle varies continuously and the centerline is curved, but since the propeller is most sensitive to conditions near the disk, the wake can be assumed straight with the skew angle defined by conditions at the disk. This skew can be observed from the simple force-velocity geometry of a momentum theory approach to the problem, as in Fig. 1. The skew angle and angle of attack are thus related by

$$\chi = \tan^{-1}[\mu \sin\alpha/(\mu \cos\alpha + v/V_T)] \tag{13}$$

and the momentum-induced velocity is[4]

$$(v/V_T)^4 + 2\mu \cos\alpha(v/V_T)^3 + \mu^2(v/V_T)^2 - (C_T/2)^2 = 0 \tag{14}$$

where $C_T = T/\rho\pi R^2 V_T^2$. Note that, particularly under the assumption of light loading, the skew angle is relatively insensitive to v/V_T except at large values of α.

With the assumptions carried over from axial propeller theory and those established for the angle-of-attack case, the physical model necessary to obtain the tip-loss factor can be constructed. The proposed model consists of a steady flow vortex wake skewed at some angle to the axis of rotation. The wake assumes a general helical shape with the loops parallel to the disk plane moving aft as a rigid surface. Because the helical loops are parallel to the disk plane, they are skewed from a normal to the centerline. The rigid wake will advance parallel to the thrust direction at a rate dictated by an advance velocity W_0/V_T, analogous to the Goldstein advance velocity[5] for axial flight. The skew can then be obtained from Eq. (13) on replacing v/V_T by W_0/V_T. However, in practice $v/V_T \cong W_0/V_T$ so that Eq. (13) can be used directly to determine skew.[4,5] Then, if the flow pattern exterior to this wake can be determined, the circulation distribution and the tip-loss factor can be obtained.

Making the same assumptions on the propeller operating characteristics as Prandtl,[3] the physical model can be similarly simplified. The propeller is assumed to have a large number of blades and to be operating at a low advance ratio. This permits the flow exterior to the vortex wake to be approximated by a flow exterior to an infinite number of slits of finite length. Because the loops of the vortex wake are parallel to the propeller disk plane and the wake centerline is skewed to the axis of rotation, the slits will be skewed from the normal to the wake centerline. This flow geometry is shown in Fig. 2.

In order to interpret the results of the proposed model in terms of Prandtl's original result for axial flight, it is necessary to show that the slit circulation distribution is symmetrical about the wake centerline. This can be accomplished by considerations of the flow pattern of Fig. 2. If the flow pattern on one side, say the upper side, of the wake centerline is due to a freestream velocity advancing from $(-\infty)$ to $(+\infty)$, then the flow pattern on the other side is due to the same freestream advancing from $(+\infty)$ to $(-\infty)$. Now select two streamlines, one on either side of the centerline, such that the mass flow rates between the centerline and strips and the selected streamlines are equal. Locate two points A and A^1 on one streamline and B and B^1 on the other such that the pairs of points are at equal radial distances r measured along the strip from the centerline. The geometry of the flow pattern shows that the slopes of the streamlines on opposite sides of the strip are equal. That is, the slope of the streamline at A equals the slope at B^1 and the slope at A^1 equals the slope at B. This establishes the velocities at A and B^1 to be equal; similarly the velocities at A^1 and

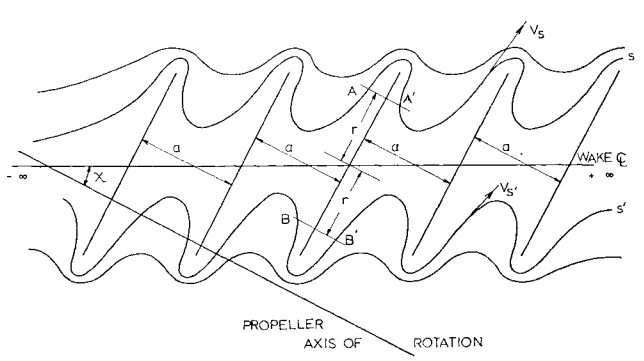

Fig. 2 Physical model to approximate flow pattern exterior to vortex wake of propeller at an angle of attack.

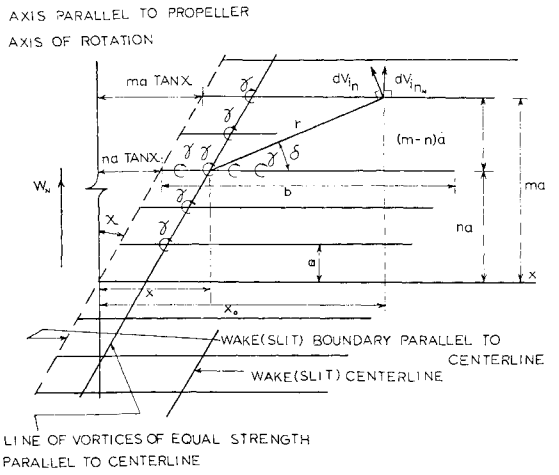

Fig. 3 Vortex geometry to approximate flow pattern.

B are also equal. Thus, the flow pattern exterior to the slits possesses a skew symmetry such that velocity differences between pairs of points at equal radii from the wake centerline are equal in magnitude and opposite in sign. This implies that the differences in velocity potential between such pairs of points are also equal and opposite. Then, if the streamline that traces the strips is considered, equal and opposite potential discontinuities at equal radii on either side of the centerline are obtained. These potential discontinuities are circulations and it is established that the slit circulation distribution is symmetrical about the wake centerline.

Since the strips are streamlines of the flow which support circulation distributions they may be replaced by sheets of distributed vorticity. A unique solution to the vorticity distribution can then be obtained by applying the boundary condition that there be no flow across the strips and the condition of symmetry of the slit circulation distribution. Integration of the vorticity distribution then gives a circulation distribution analogous to that obtained by Prandtl for the axial flight case.

The assumed vortex geometry of the strips is given in Fig. 3. Referring to this geometry, the normal component of velocity induced at a point (x_0, $ma\tan\chi$) on the mth strip by all vortices of strength γdx on n number of strips is given by

$$V_{i_N} = \frac{1}{2\pi}\sum_{n=-\infty}^{\infty}\int_{x=na\tan\chi}^{na\tan\chi+b}\frac{\gamma(x_0-x)dx}{(x_0-x)^2+a^2(m-n)^2} \tag{15}$$

This velocity must just cancel some freestream, or impact, velocity normal to the strip at the strip. Thus, at the strip,

$$W_N + V_{i_N} = 0 \tag{16}$$

becomes the statement of the boundary condition. Since the mth strip and x_0 are undefined, the boundary condition is satisfied at any point on any strip. Further, the vorticity distributions and, therefore, the bound circulation distribution on all strips are identical. Thus, for simplicity, the boundary condition is satisfied on the mth strip taken as zero so that Eq. (16) becomes

$$1+\sum_{n=-\infty}^{\infty}\int_0^{b/a}\frac{\bar\gamma(\bar x_0-\bar x-n\tan\chi)d\bar x}{(x_0-x-n\tan\chi)^2+n^2}=0 \tag{17}$$

where $\gamma = 2\pi W_N\bar\gamma$ and $x = a\bar x$. The condition of symmetry of the bound circulation about the wake centerline is given by

$$\int_0^{b/a}\bar\gamma d\bar x = 0 \tag{18}$$

and the value of the bound circulation at any point $\bar X$ is

$$\bar\Gamma = \int_0^{\bar X}\bar\gamma d\bar x \tag{19}$$

The solution of Eqs. (17) and (18) will yield the vorticity distribution along the slit and Eq. (19) then gives the bound circulation along the slit.

As previously stated, Prandtl's solution with semi-infinite strips is an approximation to the case of finite strips permitted because of the complete flow symmetry about the wake centerline. Thus, the Prandtl solution at $x/a = \infty$ must correspond to the midspan value of the finite slit solution in the limit as the slit span b becomes infinite. Then the term Γ_∞ is obtained from the finite slit model as

$$\bar\Gamma_\infty = \lim_{b/a\to\infty}\int_0^{b/2a}\bar\gamma d\bar x \tag{20}$$

$$F = \lim_{b/a\to\infty}\left[\left(\int_0^{\bar x}\bar\gamma d\bar x\right)\Big/\left(\int_0^{b/2a}\bar\gamma d\bar x\right)\right] \tag{21}$$

The tip-loss factor can be written in terms of Prandtl's solution for no skew and a correction factor due to skew by first normalizing Eq. (21) on the zero skew case. Then

$$F = F_0\left\{\frac{\lim_{b/a\to\infty}\left(\int_0^{\bar x}\bar\gamma d\bar x\Big/\int_0^{b/2a}\bar\gamma d\bar x\right)}{\left[\lim_{b/a\to\infty}\left(\int_0^{\bar X}\bar\gamma d\bar x\Big/\int_0^{b/2a}\bar\gamma d\bar x\right)\right]_{\chi=0^\circ}}\right\} \tag{22}$$

where F_0 is given by Eq. (1) and the $[\ ]_{\chi=0^\circ}$ bracketed term represents the solution to Eq. (21) for zero skew angle. The $\{\ \}$ bracketed term then represents a correction to the zero skew tip-loss factor to account for the wake skew.

The results of this analysis will give one distribution of F against x or x/a for one value of skew angle χ and this is consistent with Eq. (1). The quantity x/a is defined by Eq. (1) for the axial flight case, and since the present analysis also considers a steady flow problem with equispaced slits, Eq. (1) and its interpretation must also apply here. Hence, each distribution of F against x/a represents a infinite number of propeller circulation distributions depending on the number of blades and the propeller radius.

Application of Results to the "Direct Problem"

Assuming the tip-loss factor can be obtained from Eq. (21) or (22), the application of this result to the solution of the "direct problem" is desired. This problem assumes the physical parameters of the blade to be known and determines the loading and attendant thrust and power characteristics. Further, the problem is really an unsteady problem by the introduction of the unsteady velocity in the plane of rotation, $\mu\sin\alpha\sin\psi$, and will be treated as such here.

From the methods of Ref. 3 the following four steady flow equations can be generated for the propeller at an angle of attack:

$$\tan\phi_e = (\mu\cos\alpha + W_a/V_T)/(\bar r - W_t/V_T) \tag{23}$$

$$V_e/V_T = [(\mu\cos\alpha + W_a/V_T)^2 + (\bar r - W_t/V_T)^2]^{1/2} \tag{24}$$

$$W_a/V_T = \{-\mu\cos\alpha + [(\mu\cos\alpha)^2 + 8(\bar r - 2W_t/V_T)W_t/V_T]^{1/2}\}/4 \tag{25}$$

$$W_t/V_T = \sigma a_0(\beta-\phi_e)(V_e/V_T)/8\bar r F \tag{26}$$

Equations (23), (24), and (25) are obtained from the geometry of Fig. 4 by disregarding the unsteady aspects of the flow; Eq. (26) is obtained as a solution to Eqs. (11) and (13) utilizing $\Gamma_0 = (V_e/2)ca_0(\beta-\phi_e)$. These four equations can be solved by iterative procedures to yield the flow velocity and helix pitch angle distributions at the blade.

The unsteady velocities and pitch angle can be determined from the known steady flow distribution by assuming that conditions in the ultimate wake are the same for both the steady and unsteady flows. That is, the advance velocity of the wake W_0 is the same and the normality of the resultant induced velocity to the vortex sheet applies in both cases. Then, referring to Fig. 4,

$$\tan\phi_{\infty_u} = \tan\phi_\infty/(1+\mu\sin\alpha\sin\psi/\bar r) \tag{27}$$

$$W_{a_u} = W_a(\cos\phi_{\infty_u}/\cos\phi_\infty)^2 \tag{28}$$

$$W_{t_u} = W_t(\sin2\phi_{\infty_u}/\sin2\phi_\infty) \tag{29}$$

where

$$\tan\phi_\infty = (\mu\cos\alpha + 2W_a/V_T)/(\bar r - 2W_t/V_T) \tag{30}$$

Conditions at the blade can now be obtained from Fig. 4. The unsteady pitch angle and effective velocity are found to be

$$\tan\phi_{e_u} = (\mu\cos\alpha + W_{a_u}/V_T)/(\bar r + \mu\sin\alpha\sin\psi - W_{t_u}/V_T) \tag{31}$$

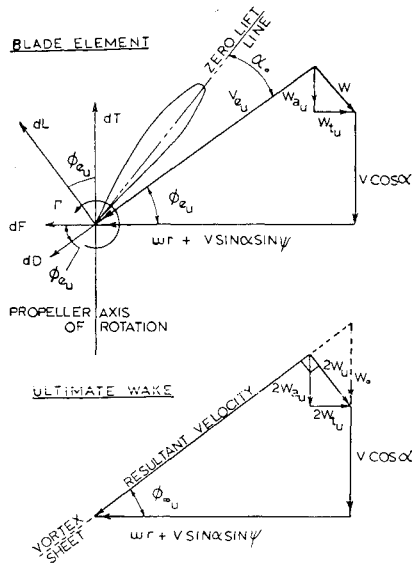

Fig. 4 Force and velocity geometry at a blade element and in the ultimate wake.

and

$$V_{eu}/V_T = (\mu \cos\alpha + W_{au}/V_T)^2 + [(\bar{r} + \mu \sin\alpha \sin\psi - W_{tu}/V_T)^2]^{1/2} \quad (32)$$

Then the average thrust and power required can be obtained from

$$C_T = \left(\frac{1}{4\pi}\right) \int_0^{2\pi} \int_{\bar{r}_h}^{1.00} \left(\frac{V_{eu}}{V_T}\right)^2 \sigma(C_l \cos\phi_{eu} - C_d \sin\phi_{eu}) d\bar{r} d\psi \quad (33)$$

and

$$C_p = \left(\frac{1}{4\pi}\right) \int_0^{2\pi} \int_{\bar{r}_h}^{1.00} \left(\frac{V_{eu}}{V_T}\right)^2 \sigma(C_l \sin\phi_{eu} + C_d \cos\phi_{eu}) \bar{r} d\bar{r} d\psi \quad (34)$$

where $C_l = a_0(\beta - \phi_{eu})$, and a_0, σ, C_d represent the known section characteristics.

The system of Eqs. (23–34) necessary to obtain the thrust and power requirements is difficult to handle analytically and the solution is best obtained by numerical means. A suggested procedure for obtaining a solution to the direct problem is as follows.

1) Number of blades, local solidity distribution, section lift curve slope and drag coefficient distribution, blade pitch angle distribution, tip-speed ratio and propeller angle of attack are known.

2) Assume momentum theory value of induced velocity or assume an operating thrust coefficient and calculate the induced velocity from Eq. (14).

3) Obtain wake skew angle from Eq. (13).

4) Obtain tip-loss factor from numerical solution to Eqs. (17, 18, and 21 or 22).

5) Iterate Eqs. (23–26) for steady flow velocity distributions.

6) Obtain unsteady distributions from Eqs. (27–32)

7) Integrate Eqs. (33) and (34) for thrust coefficient and power coefficient.

8) Recalculate induced velocity of (2) and iterate through (8) until two successive thrust coefficients compare favorably.

Necessary corrections such as compressibility or retreating blade stall can be applied and are available in the literature.[4] Note that the tip-loss factor enters into the determination of the steady flow induced velocity distribution and the bound circulation is not directly considered.

Numerical Solution to the Tip-Loss Factor

The tip-loss factor is obtained from Eqs. (17, 18, 21, and 22) by a straightforward numerical integration. Equations (17) and (18) are written in terms of finite vortices with Eq. (17) satisfied midway between successive vortices. The method requires that, if there exists k number of vortices approximating the slit distribution, there are $k - 1$ equations of the form of (17); the kth equation is given by the symmetry condition of (18). A simultaneous solution to (17) and (18) thus yields a unique vorticity distribution for specified values of wake skew angle. Equations (21) and (22) then determine the tip-loss factor and the correction F/F_0, respectively.

The numerical integration was performed on the IBM 7074 high-speed digital computer at the Pennsylvania State University Computation Center. Six values of skew angle ($\chi = 0°$, 15°, 30°, 45°, 60°, and 75°) were considered. The results showing the effect of skew on the tip-loss factor are given graphically as Figs. 5–7. Figure 5 gives the tip-loss factor F against x/a from Eq. (21), whereas Figs. 6 and 7 give the correction to the axial flight case F/F_0 against x/a from Eq. (22). Figure 7 is an expanded view of Fig. 6 in the region around $x/a = 0$, which is the region of most practical interest. Figure 5 also shows a comparison between the present analysis for zero skew and a numerical solution to Prandtl's original result of Eq. (1). The results compare in general to well within 1%.

It is believed the results are accurate over the region of practical interest, $x/a \lesssim 2$. However, some question arises at the higher values. It can be noted from Fig. 6 that the tip-loss factor becomes greater than unity for nonzero skew conditions and approaches one asymptotically from the high

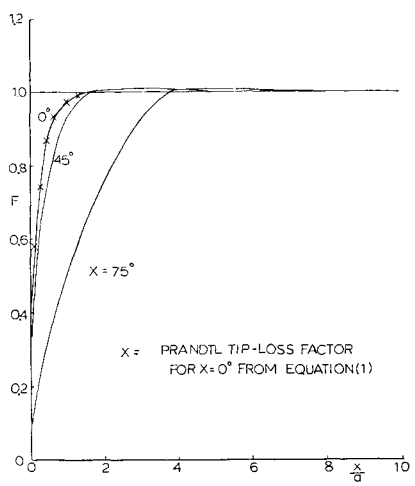

Fig. 5 Effect of wake skew on tip-loss factor.

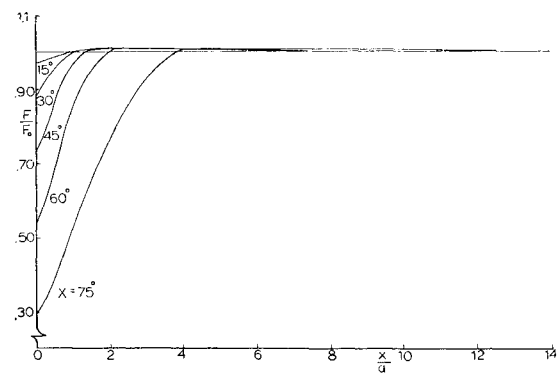

Fig. 6 Effect of wake skew on correction to prandtl tip-loss factor.

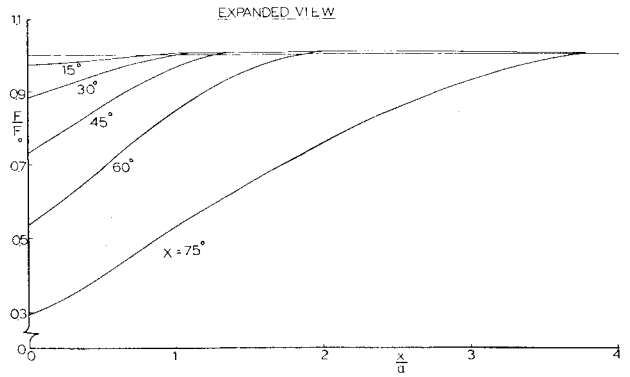

Fig. 7 Effect of wake skew on correction to prandtl tip-loss factor.

side. Although the maximum amount by which unity is exceeded is only on the order of 0.003, some question as to numerical accuracy in this region does arise. If the results are accepted as they stand, then it must be concluded that some combination of blade number and wake helix angle yields a greater circulation than does an infinite number of blades. Or, to interpret the results in a slightly different light, some combination of blade number and wake helix angle yields a greater average tangential induced velocity than does an infinite number of blades; and the physics of the problem indicates this cannot be so. Thus, there must be either some inaccuracy in the numerical integration or an extremely subtle physical situation. It is suspected that this curve should approach unity asymptotically from the low side ($F < 1$). In general, though, within the region of practical interest, the results indicate an increase in the tip-loss factor with x/a increasing, which agrees with Prandtl's solution.

Comparison of Theoretical and Experimental Results

Lack of adequate facilities prohibited any experimental program to verify the theory. For this reason the existing experimental evidence of Ref. 2 was used for comparison, the comparison being carried out for a propeller angle-of-attack range from 0° through 75°.

The four-bladed propeller investigated in the cited reference has a 5.33-ft diameter and utilized an NACA 16-series airfoil distribution along the blade span. The blade pitch angle at the 0.75 radius was 30°. The blade-form curves for the propeller are given in Fig. 2 of the reference. The necessary section data for the NACA 16-series airfoil were obtained from Refs. 3 and 7.

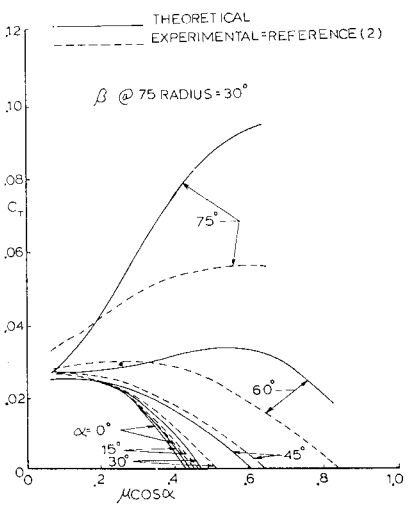

Fig. 8 Effect of angle of attack on thrust.

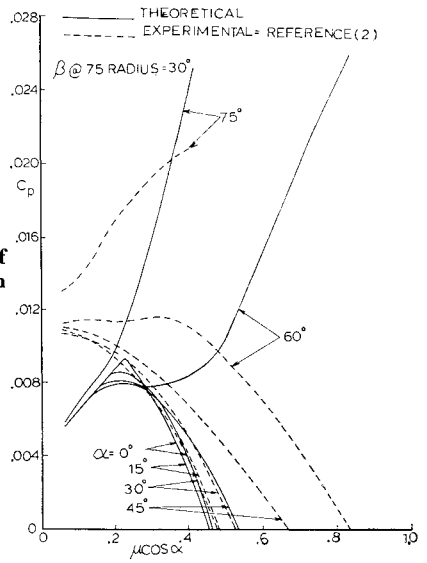

Fig. 9 Effect of angle of attack on power.

The theoretical results were obtained by numerical integration on the IBM 7074 digital computer. The calculated and experimental thrust and power coefficients are shown in Figs. 8 and 9, respectively. The theoretical values are again shown in expanded views, with lines of constant tip-speed ratio superimposed in Figs. 10 and 11. Reynolds' number effects were neglected. Since the tests of Ref. 2 were run to maintain the propeller blade sections below the critical Mach Number, compressibility considerations should be relatively unimportant.

In general, the trends shown by the theoretical variations are favorable in that they indicate the same general forms as do the experimental results. The C_T variations are, for the most part, better than the C_p variations. The power is greatly underestimated at low values of $\mu \cos\alpha$ for all angles of attack, and the $\alpha = 60°$ curve increases drastically at high values of $\mu \cos\alpha$, which contrasts sharply to the experimental evidence. In general, the thrust and power are both overestimated to some degree at high values of α and $\mu \cos\alpha$ and underestimated at the lower values.

If the expanded views of Figs. 10 and 11 are considered, a certain degree of verification of the theory can be obtained from the lines of constant μ. The $\mu = 0.3$ line can be assumed representative of present-day rotary wing operation. The $\mu = 1.00$ line might be considered as an upper limit on existing rotary wing speeds for the foreseeable future. These

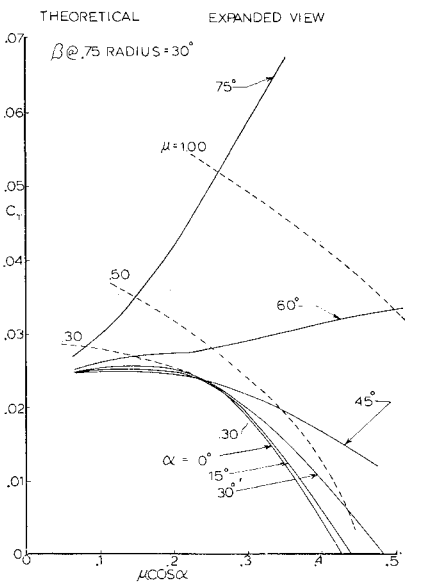

Fig. 10 Effect of angle of attack on thrust.

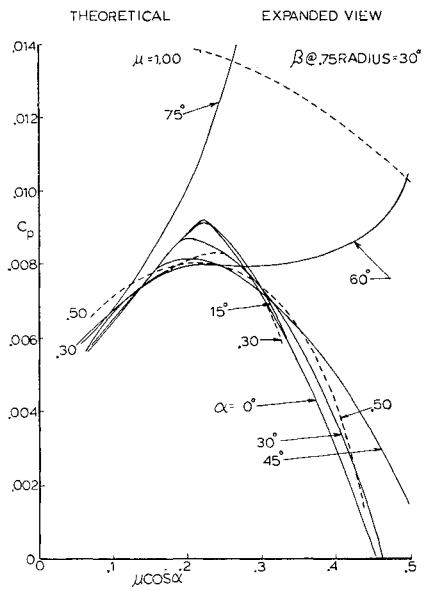

Fig. 11 Effect of angle of attack on power.

assumptions are reasonable if it is recalled that a propeller operates at high $\mu \cos\alpha$ values at low angles of attack and low $\mu \cos\alpha$ values at high angles of attack. Now if the regions bounded by these lines are considered, fair agreement does exist between theory and experiment. Excepting the underestimated power at low values of $\mu \cos\alpha$, the region of greatest error lies outside the $\mu = 1.00$ line; hence, the major discrepancies become a problem of academic, rather than practical, interest.

The error accumulated in the theoretical results comes from varied sources. Sources of minor error include the numerical integration, the manual scaling of the experimental data and blade-form curves from Ref. 2, the empirical relations for maximum lift coefficient and minimum drag coefficient, the assumed constant linear lift curve slope, and neglect of Reynolds' number effect.

The theory itself represents a possible source of error. Since the assumed physical model is essentially the same as the original Prandtl model, both should have the same limits of accuracy. Thus, it might be expected that the accuracy of the developed analysis will increase with increasing number of blades or decreasing advance ratio. Further, the analysis is a quasi-steady form with no attempt made to account for the effect of the shed wake; associated error would increase with increases in $(\mu \cos\alpha, \alpha)$.

Since thrust predictions are reasonably valid but power predictions appear quite inaccurate, some question as to the estimated C_d of the blade section is raised. Investigation of the blade C_l distributions indicates operation near static $C_{l\max}$ at both low and high values of $(\mu \cos\alpha, \alpha)$ which corresponds to low inflow values. The 16-series airfoil exhibits an exceedingly sharp drag rise just before the stall which makes C_d estimates in this range dubious. It is believed this contributes more than might normally be expected to the poor C_p prediction at low values of $(\mu \cos\alpha, \alpha)$.

Error at high values of $(\mu \cos\alpha, \alpha)$ can be attributed in part to an only elementary inclusion of reverse flow effects. The in-plane component of velocity was checked repeatedly and if reverse flow was indicated the airfoil characteristics were obtained as if the section was in a normal operating range and the proper signs applied to the differential C_T and C_p. Some data[8] for airfoils at extreme angles of attack do exist; but extrapolating this into reverse flow, a negative angle of attack regime, for the generally erratic 16-series airfoil is questionable at best.

At high values of $(\mu \cos\alpha, \alpha)$ it is doubtful if static values apply. Recent work[9] shows the dynamic behavior of airfoils near static $C_{l\max}$ to exhibit increases in C_l and decreases in C_d beyond the static values. Had this type of data for the 16-series airfoil been employed, a reduction in the estimated C_p would have been noted. Further, dynamic considerations in reverse flow might well improve negative C_l's, which will act to decrease the C_T estimates at large $(\mu \cos\alpha, \alpha)$.

Summary and Conclusions

The foregoing analysis presents an extension of the Prandtl propeller analysis into the extreme angle-of-attack regime. The assumptions regarding the mathematical model are consistent with those of the Prandtl-Goldstein model. The result is obtained in terms of a tip-loss factor which shows a dependency on wake skew; this tip-loss factor, like the Prandtl axial flight result, is interpreted as an averaging factor on the bound circulation distribution to account for finite blade spacing.

The tip-loss factor is applied to a quasi-steady determination of propeller thrust and power characteristics. Comparison with experimental evidence indicates the method can estimate such performance through a large angle-of-attack range provided the necessary physical data for the selected airfoil sections can be determined.

References

[1] Heyson, H. H. et al, "Induced Velocities near a Lifting Rotor with Nonuniform Disc Loading," TR-1319, 1957, NACA.

[2] McLemore, H. C. et al., "Aerodynamic Investigation of a Four-Blade Propeller Operating through an Angle-of-Attack Range from 0° to 180°," TN-3228, June 1954, NACA.

[3] McCormick, B. W., Jr. et al, "A Study of Torpedo Propellers—Part 1," ORL, Serial No. 16597, March 1956.

[4] McCormick, B. W., Jr., *Aerodynamics of V/STOL Aircraft*, Academic Press, 1967.

[5] Goldstein, S., "On the Vortex Theory of Screw Propellers," *Proceedings of the Royal Society*, Series A, Vol. 123, 1929, p. 440.

[6] Miller, R. H., "Rotor Blade Harmonic Air Loading," Paper 62-82, Jan. 1962, IAS.

[7] Lindsey, W. F. et al, "Aerodynamic Characteristics of 24 NACA 16-series Airfoil at Mach Numbers Between 0.3 and 0.8," TN-1546, Sept. 1948, NACA.

[8] Critzos, C. C. et al, "Aerodynamic Characteristics of NACA 0012 Airfoil Sections at Angles-of-Attack from 0° to 180°," TN-3361, Jan. 1955, NACA.

[9] Liiva, J. and Davenport, F. J., "Dynamic Stall of Airfoil Sections for High-Speed Rotors," presented at the 24th Annual National Forum of the American Helicopter Society, May 1968.